

# Surface-Controlled Gas-Phase Deposition and Characterization of Highly Dispersed Vanadia on Silica

Jetta Keranen,<sup>†,‡</sup> Claude Guimon,<sup>§</sup> Eero Iiskola,<sup>‡</sup> Aline Auroux,<sup>\*,†</sup> and Lauri Niinisto<sup>‡</sup>

*Institut de Recherches sur la Catalyse, UPR (CNRS) 5401, 2 avenue Albert Einstein,*

*F-69626 Villeurbanne Cedex, France, Laboratory of Inorganic and Analytical Chemistry, Helsinki University of Technology, P.O. Box 6100, FIN-02015 Espoo, Finland, and Laboratoire de Physico-Chimie Moléculaire, UMR (CNRS) 5624, Université de Pau et des Pays de l'Adour, 2 avenue du Président Angot, F-64053 Pau Cedex 9, France*

*Received: March 31, 2003*

Highly dispersed  $V_2O_5/SiO_2$  materials were successfully synthesized using the atomic layer deposition (ALD), by sequentially applying surface-saturating reactions of volatilized vanadyl triisopropoxide and oxygen with the silica surface. The controlled and reproducible chemisorption-based growth of vanadia on silica occurred in a temperature range from 363 to 393 K, as confirmed by elemental analyses and DRIFTS measurements. The precursor deposition progressed via both mono- and bidentate surface species, depending on the silica pretreatment temperature. Upon increase of the silica preheating temperature from 473 to 1023 K, i.e., decreasing the number of isolated OH groups, the vanadium densities diminished from 2.0 to 1.1 V at/nm<sup>2</sup><sub>support</sub>. The maximum dispersion of vanadia ( $\sim 2.3$  V at/nm<sup>2</sup><sub>support</sub>) was attained by two consecutive precursor binding-oxidation cycles on silica pretreated at 873 K. Analogous liquid-phase-impregnated catalysts were prepared for comparison, and the structure and dispersion of the catalysts were studied by N<sub>2</sub> adsorption, XRD, XPS, and Raman spectroscopy. The results showed that the properties of the silica-supported vanadia catalysts were strongly affected by the preparative method. The ALD catalysts with loadings between 1.0 and 2.3 V at/nm<sup>2</sup><sub>support</sub> consisted of highly dispersed isolated VO<sub>4</sub> species, whereas in the corresponding impregnated catalysts, V<sub>2</sub>O<sub>5</sub> crystallites were formed, in addition to the monomeric vanadia species. The vanadia deposition either by ALD or impregnation created both Lewis and Brønsted surface acid sites of weak and medium strength, as detected by ammonia adsorption XPS and microcalorimetry. However, the better dispersion of the surface vanadia species in the catalysts prepared by the gas-phase route led to a 30% higher number of surface acid sites.

## 1. Introduction

Silica-supported vanadia catalysts find applications in several catalytic processes, i.e., in methane oxidation to formaldehyde<sup>1–3</sup> and in oxidative dehydrogenation of ethane to ethylene<sup>4</sup> or that of ethanol to acetaldehyde.<sup>5</sup> Traditionally, the  $V_2O_5/SiO_2$  catalysts have been prepared by aqueous-phase impregnation using solutions containing ammonium metavanadate NH<sub>4</sub>VO<sub>3</sub>.<sup>6–8</sup> Due to the chemical inertness of silica, this preparative method often leads to crystalline V<sub>2</sub>O<sub>5</sub> even at a low vanadia coverage ( $\sim 1.0$  atoms per nm<sup>2</sup> of support).<sup>8</sup> However, the dispersion of the surface vanadia species can be maximized by using metallo-organic precursors for the preparation.<sup>5,8–10</sup> Under carefully optimized conditions, the growth proceeds selectively and homogeneously by chemisorption, i.e., by formation of covalent bonds between the precursor and pre-controlled surface adsorption sites.<sup>5,9,11,12</sup> Moreover, the gas-phase preparation approach utilizes the enhanced reactivity of the precursor and the absence of solvent effects in comparison to the liquid-phase grafting.<sup>12</sup>

Vanadyl triisopropoxide VO(OPr<sup>i</sup>)<sub>3</sub><sup>10,13–18</sup> has been previously used mainly in liquid phase for the preparation of highly

dispersed silica-supported vanadia materials. For example, Wachs and co-workers<sup>1,2,10,13,19</sup> and Scharf et al.<sup>15</sup> have applied the incipient-wetness impregnation with vanadyl triisopropoxide solution for the synthesis of these type of catalysts. However, only a few papers deal with the binding of gaseous VO(OPr<sup>i</sup>)<sub>3</sub> onto the surface hydroxyl groups of silica. The growth of vanadia onto silica using gas-phase deposition route has been studied in the literature by Nickl et al.<sup>14</sup> and Rice et al.<sup>16,17</sup> It should be noted, however, that in both of the cases, the adsorption had been carried out at room temperature, where the risk of physisorption is greater and the gas–solid reaction is less surface controlled. In addition, no thorough determination of the influence of the deposition parameters, e.g., the pretreatment temperature and amount of silica, the amount of vanadyl triisopropoxide precursor, and the temperature of the chemisorption, has been carried out. Also, detailed information on the binding mode of the precursor, on the controllability, and on the reproducibility of the surface reaction as a function of the number of precursor binding-oxidation cycles is missing in the literature.

The atomic layer deposition (ALD) technique is a chemisorption-based, gas-phase preparative method for thin films and overlayers.<sup>11,20–22</sup> The growth of metal oxides is achieved by sequential surface-saturating reactions of gaseous precursors with the support. The adsorption-controlled deposition allows

\* To whom correspondence should be addressed. Tel: +33-47244-5343. Fax: +33-47244-5399. E-mail: auroux@catalyse.cnrs.fr.

<sup>†</sup> Institut de Recherches sur la Catalyse.

<sup>‡</sup> Helsinki University of Technology.

<sup>§</sup> Université de Pau et des Pays de l'Adour.

enhanced species dispersion and uniformity on the support surface.<sup>11,23</sup> Recently, we have applied the ALD technique to the preparation of submonolayer vanadia catalysts supported on silica, titania, and titania/silica, starting from the  $\text{VO}(\text{OPr})_3$  precursor.<sup>18</sup> In the present study, the preparation of highly dispersed vanadia/silica materials by the ALD technique and using the vanadyl triisopropoxide precursor is examined in detail. The ideal processing conditions for the precursor chemisorption on silica pretreated at different temperatures were first determined by elemental analyses and inert atmosphere DRIFTS. Increasing amounts of vanadia were then deposited onto the supports by sequential surface reactions of precursor and oxygen. The catalysts were characterized by  $\text{N}_2$  adsorption and X-ray diffraction (XRD) techniques. Raman spectroscopy was employed for structural examination and X-ray photoelectron spectroscopy for evaluating the dispersion of the active phase on the support. To probe the surface reactivity and to obtain qualitative information on the nature of the acid sites, XP spectra were collected after ammonia adsorption. Moreover, microcalorimetry experiments of  $\text{NH}_3$  adsorption were performed in order to determine the number, strength, and strength distribution of surface acid sites. Some conventional aqueous-phase impregnated samples were also prepared and characterized for comparison with the ALD catalysts.

## 2. Experimental Section

**2.1. Catalyst Preparation.** The silica support used in the preparations was EP10 from Crosfield Ltd. (primary particle size  $\sim 110\ \mu\text{m}$ ,  $\text{Na}_2\text{O} < 500\ \text{ppm}$ ). Prior to the deposition process, the support was pretreated in air for 16 h at 473, 723, 873, and 1023 K in a muffle furnace to remove the physisorbed water and to stabilize the adsorption sites of the support.<sup>11</sup> These silica supports will be here referred to as  $\text{SiO}_2$  473 K,  $\text{SiO}_2$  723 K,  $\text{SiO}_2$  873 K, and  $\text{SiO}_2$  1023 K. The pretreatment at temperatures between 473 and 873 K preserved the surface area, pore volume, and average pore diameter of silica, with values of  $301 \pm 8\ \text{m}^2/\text{g}$ ,  $1.2\ \text{cm}^3/\text{g}$ , and  $19\text{--}20\ \text{nm}$ , respectively. After treatment at 1023 K, however, the specific surface area diminished to  $286 \pm 7\ \text{m}^2/\text{g}$  and the pore volume to  $1.1\ \text{cm}^3/\text{g}$ , whereas the average pore diameter remained unchanged. A 5-g sample of the support was loaded into the fixed-bed quartz chamber of a flow-type ALD reactor<sup>23</sup> (F-120, ASM Microchemistry Ltd.), and the temperature was raised to 473 K for 16 h for the silica pretreated at 473 K and to between 363 and 433 K for 2–3 h for the supports pretreated at 723, 873, and 1023 K. This further heat treatments were carried out to remove from the pretreated support any humidity possibly condensed during the short manipulation and to ensure the stabilization of the support adsorption sites.<sup>11</sup> The reactor was maintained in low vacuum (pressure 1–3 kPa) and purged continuously with a nitrogen flow (3 L/h). The vanadium precursor used was a liquid vanadyl triisopropoxide  $\text{VO}(\text{OC}_3\text{H}_9)_3$  (Strem Chemicals Inc., purity 98+%), volatilizable from 363 to 383 K. The reaction between  $\text{VO}(\text{OPr})_3$  and silica pretreated at 873 K was investigated at every 10 K between 363 and 433 K by letting the precursor-carrier gas flow (3 L/h) pass downward through the support bed during 5–8 h. The precursor was used in excess, i.e., around 2.5 mmol per gram of support ( $\text{g}_{\text{sup}}$ ), to ensure a complete saturation of the support.<sup>11</sup> Finally, the solids were purged with nitrogen for 2 h at the reaction temperature and calcined in-situ in oxygen at 773 K for 11 h.

The influence of the pretreatment temperature of silica on the vanadium surface species and their amount was studied at the reaction temperature of 363 K. The precursor quantity used

was 3.5 mmol/ $\text{g}_{\text{sup}}$  for the supports pretreated at 473 and 723 K and 2–3.5 mmol/ $\text{g}_{\text{sup}}$  for the support pretreated at 1023 K. The complexes on silica pretreated at 723 and 1023 K were calcined, as described above, at 723 and 773 K, respectively, and the solids were subjected to a further examination.

To increase the deposited amount of vanadium and to obtain information of how the vanadia layer already present influences the controllability of the reaction, successive precursor-oxygen cycles on silica pretreated at 873 K were performed from one to four times at a deposition temperature of 383 K. To prevent surface hydration, the samples were kept under inert conditions between the cycles.

In addition to the ALD samples, two conventional impregnated silica supported vanadia samples were prepared to examine the influence of the preparative method on the characteristics of the catalysts. The silica support was impregnated with aqueous solutions of ammonium metavanadate (Strem Chemicals, purity 99%) and oxalic acid (Prolabo, purity 99%). The solutions were prepared by heating the mixed slurries of  $\text{NH}_4\text{VO}_3$  and  $\text{C}_2\text{O}_4\text{H}_2 \cdot 2\ \text{H}_2\text{O}$  (ratio of 1:2) at 333 K. The solids were dried for 24 h at 383 K and subsequently calcined following the same procedure as for the ALD catalysts, i.e., in oxygen at 773 K for 11 h.

**2.2. Catalyst Characterization.** The amount of vanadium in the samples was determined by ICP-AES (Spectroflame-ICP D, Spectro) and the amount of carbon by total combustion in oxygen followed by an acidimetric coulometry measurement. The element contents are given throughout the text as surface densities in atoms per  $\text{nm}^2$  of support ( $\text{at}/\text{nm}^2_{\text{sup}}$ ) and as weight percentages (wt-%). In the calcined catalysts, the atom densities were calculated based on the generalization that the vanadia phase corresponds to  $\text{V}_2\text{O}_5$ . In the noncalcined samples, the forms of the surface species were derived from the carbon/vanadium (C/V) or ligand/vanadium (L/V) ratios. The L/V ratio after several deposition cycles was obtained by taking into account only the amount of vanadium (and carbon) added onto the surface after previous oxidation. A verification of the proposed surface species formed after binding of the precursor on support was done by molecular modeling, using the Alchemy 32 program (version 2.0, Tripos Inc.).

The specific surface area ( $S_{\text{BET}}$ ) as well as pore size and diameter were measured by nitrogen adsorption at 77 K on the catalysts desorbed under vacuum at 623 K for 3.5 h. Diffuse reflectance infrared spectra of silica-supported samples prepared by ALD were recorded under nitrogen atmosphere at room temperature using a Nicolet Impact 400 D FTIR spectrometer. The measurements were carried out for the freshly prepared samples both after deposition at different temperatures and after subsequent oxidation by transferring the samples inertly into the DRIFTS chamber placed in a glovebox. The wavenumber range used in the measurements was from 400 to  $4000\ \text{cm}^{-1}$  and the spectral resolution and number of scans were  $2\ \text{cm}^{-1}$  and 64, respectively.

The X-ray diffraction spectra were recorded in a Bruker D5005 diffractometer (50 kV, 35 mA) between the Bragg angles ( $2\theta$ ) from 3 to  $80^\circ$  using a monochromated  $\text{Cu}\ \text{K}\alpha$  ( $\lambda = 0.015418\ \text{nm}$ ) radiation source.

The Raman spectroscopy measurements were carried out in a Dilor XY spectrometer connected to an Olympus BH-2 microscope (objective G = 50). The samples were excited by the 514.5 nm line of an argon ion laser (Spectra Physics) and the laser power was adjusted to 80 mW in order to have a 6–8 mW power when measured at the sample. Samples in the range of 20–80 mg (as a function of the density) were placed in a

special quartz microcell ( $50 \times 25 \times 6$  mm), manufactured from two parallel microscope plates, and were pretreated at 673 K for 0.5 h in dry oxygen flow to dehydrate the samples. The in- and outlets of the cell were sealed off and the spectra were collected at room temperature between 100 and  $1100\text{ cm}^{-1}$  with a resolution of  $3.0\text{ cm}^{-1}$ . The accumulation time varied from 300 to 600 s, depending on the focused sample, and was normalized to 420 s for the analyses. The homogeneity of the catalysts was verified by focusing the analysis spot (diameter  $1\text{ }\mu\text{m}$ ) through the sample at several points.

The X-ray photoelectron spectra were measured with a SSI 301 instrument equipped with a hemispherical electron analyzer and an Al anode (Al K $\alpha$  = 1486.6 eV) powered at 100 W. The residual pressure in the analysis chamber was  $5 \times 10^{-8}$  Pa. The charge effects were controlled by flooding the samples with low-energy electrons (5 eV). The wide binding energy (BE) spectra were collected at 150 eV and the high-resolution regional spectra of V2p<sup>3/2</sup>, O1s, Si2p, and N1s lines at 50 eV analyzer pass energy. The quantitative analyses of atomic ratios were carried out applying appropriate Scofield factors.<sup>24</sup> Nonlinear least-squares curve fitting (NLLSCF) was used to adjust the experimental curves to the mixture of Gaussian (80%) and Lorentzian (20%) curves. The binding energies were referenced to Si2p line of the support at 103.5 eV, the accuracy of the binding energy positions being  $\pm 0.2$  eV. The samples were activated overnight under helium at 673 K (1 K/min) and subsequently exposed to NH<sub>3</sub> at 353 K. The adsorption was followed by desorption during 1 h under helium at the same temperature. The XPS measurements were performed at room temperature, preserving inert conditions during all sample-handling steps.

The NH<sub>3</sub> adsorption microcalorimetric study was carried out at 353 K in a heat flow calorimeter (C80, Setaram) coupled to a gas handling and volumetric system.<sup>25</sup> A Barocel capacitance manometer was employed for pressure control. The NH<sub>3</sub> gas (Air Liquide, purity >99.9%) used for the measurements was purified by freeze–pump–thaw cycles. Samples of about 100 mg were pretreated in a quartz calorimetric cell at 673 K for 12–14 h in air and then for 2 h in a vacuum at the same temperature. Various thermodynamic and volumetric parameters,<sup>25</sup> e.g., the initial ( $Q_{\text{init}}$ ), differential ( $Q_{\text{diff}}$ ) and integral ( $Q_{\text{int}}$ ) heats of adsorption and the total adsorbed volume of ammonia ( $V_T$ ), were measured by sequentially loading small doses of ammonia gas onto the catalyst. The adsorption was continued until the end of chemisorption process in an equilibrium pressure of  $\sim 133$  Pa.<sup>25</sup> The reversibly adsorbed NH<sub>3</sub> molecules were removed by pumping the sample for 0.5 h at the same temperature, and to calculate the irreversible adsorbed amount ( $V_{\text{irr}}$ ), illustrating the number of strong acid sites, a readsorption was carried out at 353 K.

### 3. Results and Discussion

**3.1. Preparation of the Catalysts.** *3.1.1. Binding of the Precursor on Silica Pretreated at 873 K.* Chemical Analysis. It was possible to carry out the surface-controlled adsorption of vanadyl triisopropoxide VO(OPr)<sub>3</sub> onto silica pretreated at 873 K in a vacuum conditions (1–3 kPa) at temperatures between 363 and 393 K.<sup>26</sup> The so-called “ALD growth”<sup>11,23,26</sup> provided at least macroscopic homogeneity in the deposition<sup>11</sup> as highly equal vanadium quantities of  $1.33 \pm 0.05$  V at/nm<sup>2</sup><sub>sup</sub> were obtained throughout the silica fixed-bed, as seen in Figure 1.<sup>26</sup> In addition, the reproducibility of the growth<sup>11,23,26</sup> was confirmed to be excellent ( $< \pm 0.05$  V at/nm<sup>2</sup><sub>sup</sub>) by four duplicate runs at 383 K.

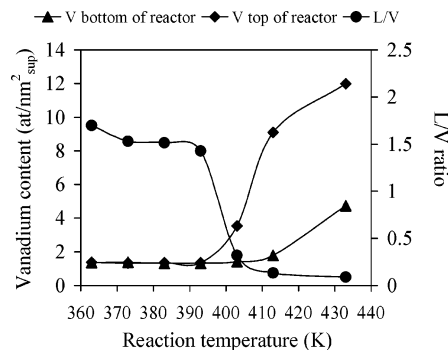


**Figure 1.** Influence of the reaction temperature on vanadium content (top and bottom of the reactor bed) and ligand/vanadium ratio (top of the reactor bed) when the precursor VO(OPr)<sub>3</sub> is bound onto silica pretreated at 873 K.

In the same temperature range, the carbon/vanadium (C/V) ratio calculated from the corresponding concentrations at the upper part of the bed decreased from 5.0 to 4.3. Thus, the ligand/vanadium ratio (L/V) in the complex attached to the silica surface decreased from 1.7 to 1.4 (Figure 1), suggesting that the binding occurred with a loss of either one ( $L/V = \sim 2$ ) or two ( $L/V = \sim 1$ ) isopropoxide precursor ligands out of the original three.

When the temperature of the reaction was raised to 403 K, a partial decomposition started to occur as observed from the increasing vanadium content and the decreasing L/V ratio at the upper part of the ALD reactor bed (Figure 1).<sup>11,23,26</sup> Further increase of the temperature of the quartz chamber up to 413 and 433 K caused the precursor excess to strongly decompose onto the silica surface and the growth started to resemble CVD, i.e., a thermal decomposition type of growth. The vanadium contents both at the top and bottom parts of the fixed-bed increased vigorously while the L/V ratio approached a zero value (Figure 1). Additionally, some precursor decomposition may have occurred already in the vapor phase, as the gas feeding lines were colored to dark violet due to the vanadium pigment.

The extension of the reaction temperature range toward lower values was found to be less practical due to the slower evaporation rate of the isopropoxide precursor. Indeed, as reported recently by Badot et al.<sup>27</sup> for thin films of vanadium oxide, the surface-controlled ALD growth from the vanadyl triisopropoxide occurred even at temperatures near room temperature (323 K), but the limiting factor was the insufficient volatilization of the precursor at low temperatures. When considering lower reaction temperatures, the risk of physisorption of the precursor should also be taken into account in addition to the longer deposition time needed.

**DRIFTS Measurements.** The temperature range for controlled binding of the precursor onto silica was also verified by inert diffuse reflectance FTIR measurements at the wavenumber range from 400 to  $3800\text{ cm}^{-1}$ . Figure 2A presents the DRIFTS patterns for the samples taken from the top of the reactor bed, while Figure 2B displays the spectra for those taken from the bottom part.

For the silica pretreated at 873 K (Figure 2, parts A, sample g, and B, sample g), the strong band observed at  $3745\text{ cm}^{-1}$  ( $\nu(\text{O}-\text{H})$ ) can be assigned to the isolated (free) silanols,<sup>28–30</sup> whereas hydrogen bonded (bridged) silanols gave rise to a weak and broad band at  $\sim 3700\text{ cm}^{-1}$  ( $\nu(\text{O}-\text{H} \cdots \text{O})$ ).<sup>28,29</sup> The weak band at  $\sim 980\text{ cm}^{-1}$  is caused by the Si–O vibration of the isolated Si–OH groups.<sup>31</sup> However, this band is partly overlapped by the one at  $\sim 1000\text{ cm}^{-1}$   $\nu(\text{Si}-\text{O}-\text{Si})$ , which is due to the formation of surface siloxanes (Figure 2, parts A, sample



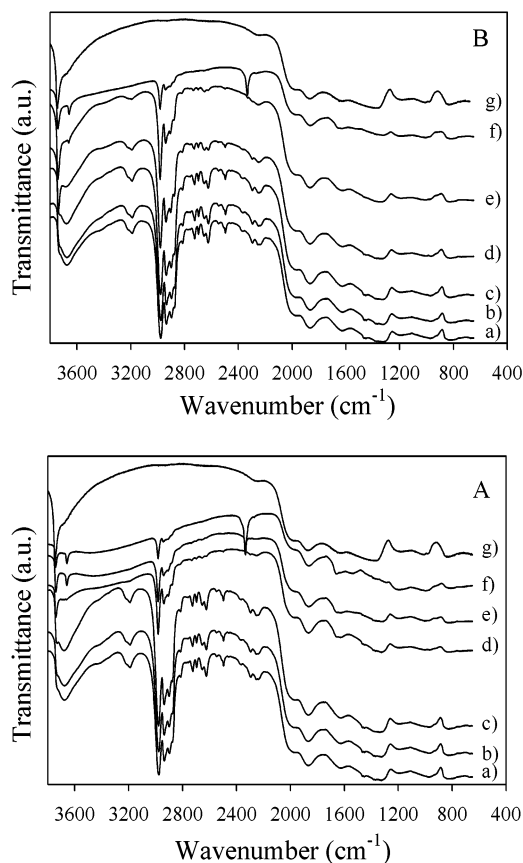


**Figure 2.** DRIFTS patterns after precursor deposition on silica pretreated at 873 K at (a) 363 K, (b) 383 K, (c) 393 K, (d) 403 K, (e) 413 K, and (f) 433 K. For comparison, the pattern of silica support is presented in (g). Samples are taken from the top (A) and bottom (B) of the reactor bed.

g, and B, sample g).<sup>28,31,32</sup> The bands at  $\sim 1250$ – $1020$   $\text{cm}^{-1}$  and  $\sim 750$ – $850$   $\text{cm}^{-1}$  are due to the asymmetric  $\nu_{\text{as}}(\text{Si}-\text{O}-\text{Si})$  and symmetric  $\nu_{\text{s}}(\text{Si}-\text{O}-\text{Si})$  stretching modes of the silica lattice, respectively.<sup>30–32</sup>

Controlled chemisorption of the precursor onto the silica surface at temperatures between 363 and 393 K gave rise to several bands in the C–H vibration region clearly identifiable as the vibration modes of isopropoxide, which is bound as a ligand to vanadium. The surface site saturation<sup>11,23,26</sup> of silica both at the top and at the bottom parts of the support bed was seen from the consumption of the free Si–OH groups at  $3745$   $\text{cm}^{-1}$  and  $\sim 980$   $\text{cm}^{-1}$  (Figure 2, parts A, samples a–c, and B, samples a–c).<sup>28–30</sup> Intense symmetric and asymmetric methyl C–H stretching vibrations were observed at wavenumbers 2882, 2932, and 2974  $\text{cm}^{-1}$ , respectively.<sup>16,33–34</sup> On the other hand, weak symmetric and asymmetric methyl C–H deformation vibrations were detected at  $1367/1381$   $\text{cm}^{-1}$  and  $1452/1467$   $\text{cm}^{-1}$ , respectively.<sup>16,33–34</sup> A methyne C–H bending band arose at  $1332$   $\text{cm}^{-1}$  (Figure 2, parts A, samples a–c, and B, samples a–c).<sup>33</sup> At the reaction temperature of 393 K, the sensitive FTIR technique also showed slight change in the reaction mode when the peak at  $3745$   $\text{cm}^{-1}$  due to non-hydrogen bonded silanols<sup>28–30</sup> appeared in the spectrum of the upper bed sample (Figure 2A, sample c). However, no changes in the vanadium contents were observed yet at this temperature, as reported above (Figure 1).

When the reaction temperature was raised from 403 to 433 K, the isopropoxide vibrations drastically decreased for the upper bed samples (Figure 2A, samples d–f). The exposed peak of isolated Si–OH groups at  $3745$   $\text{cm}^{-1}$  confirmed a heterogeneous and incomplete coverage of the surface by the attached

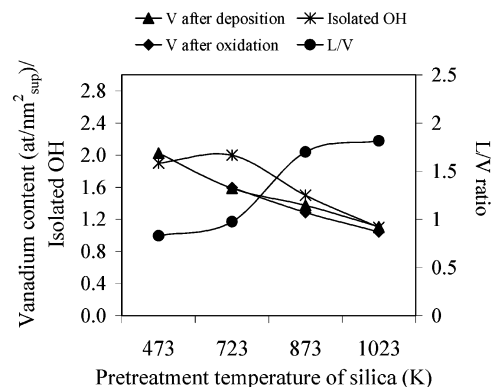


**Figure 3.** Influence of the pretreatment temperature of silica on the average vanadium contents (after deposition and oxidation) and ligand/vanadium ratio (after deposition) when the precursors  $\text{VO}(\text{OPr})_3$  and oxygen are bound onto silica pretreated at 473, 723, 873, and 1023 K. The number of isolated OH groups versus pretreatment temperature is derived from the literature.<sup>11,32,40</sup>

vanadium precursor complex. Moreover, the excess decomposition of precursor masked the intensity of the broad stretching bands of the silica support at low wavenumbers and created medium intensity peaks (Figure 2A, samples e and f) at  $3660$  and  $2334$   $\text{cm}^{-1}$ . The former band was due to  $\nu(\text{O}-\text{H})$  of vanadia surface species, and the latter can be assigned to carbon–oxygen vibrations of decomposition products.<sup>9</sup> All of these changes in the DRIFTS patterns, although being less pronounced, were observed also for the samples taken from the bottom part of the reactor bed (Figure 2B, samples d–f).

The vanadium complex formed on silica was rather stable even after several weeks of storage at room temperature under an inert atmosphere as no decomposition reaction had occurred, verified by DRIFTS measurements. However, Schraml-Marth et al.<sup>33</sup> have reported that the vanadyl triisopropoxide impregnated onto a more chemically active titania support was less stable even under inert conditions and that a sign of degradation, viz., peak of chemisorbed acetone at  $1680$   $\text{cm}^{-1}$ , could be detected within a week from the preparation.

**3.1.2. Controlled Binding of the Precursor on Silica Pretreated at Different Temperatures.** The heat pretreatment of silica, which allows the stabilization of the density, character, and type of the surface bonding sites is a prerequisite for a controlled ALD growth.<sup>11</sup> Well-characterized surface sites also allow a detailed examination of the possible surface reactions.<sup>11</sup> The adsorption sites data determined by  $^1\text{H}$  NMR measurements for silica EP10 pretreated at different temperatures are well-reported in the literature.<sup>11,29,35</sup> The total number of OH groups per  $\text{nm}^2$  of silica decreases rather linearly from 6.5 to 1.1 OH/ $\text{nm}^2$  when increasing the temperature of pretreatment from 473 to 1023 K.<sup>29</sup> The number of isolated OH groups, which act as main adsorption sites, is  $\sim 2$  OH/ $\text{nm}^2$  for silica pretreated at 473–723 K,  $\sim 1.5$  OH/ $\text{nm}^2$  for silica pretreated at 873 K, and  $\sim 1.1$  OH/ $\text{nm}^2$  for silica pretreated at 1023 K.<sup>11,29</sup> The formation of siloxane bridges Si–O–Si, which can act as dissociative bonding sites in the case of highly reactive precursors, starts at pretreatment temperatures above 723 K.<sup>11</sup>

**Chemical Analysis.** The influence of the support pretreatment temperature on the type of vanadium surface species and amount of vanadium was studied at 363 K. This low reaction temperature was chosen to exclude the possibility of thermal decomposition of the precursor during the ALD process. Figure 3 presents the average vanadium contents ( $\text{at}/\text{nm}^2_{\text{sup}}$ ) after the precursor binding and oxidation cycles as well as ligand/vanadium ratios (L/V) as a function of the pretreatment

temperature of silica. Figure 3 also shows the correlation of the isolated OH groups and the silica pretreatment temperature.

When increasing the pretreatment temperature of the support from 473 to 1023 K, the surface vanadium concentration decreased rather linearly from 2.0 to 1.1 V at/nm<sup>2</sup><sub>sup</sub> as seen in the Figure 3. The vanadium amounts were highly equal ( $< \pm 0.1$  V at/nm<sup>2</sup><sub>sup</sub>) throughout the silica support fixed-bed and followed the number of main adsorption sites (isolated OH groups) (Figure 3). This dependence on the isolated OH groups is in accordance with the results of a comparative study of several metal precursors for ALD processes, presented in the review articles by Haukka et al.<sup>11</sup> However, a clear change in the ligand/vanadium ratio (L/V) of the vanadyl isopropoxide surface complex can be seen by increasing the support pretreatment temperature from the low values (473 and 723 K) to the high values (873 and 1023 K) (Figure 3). For the lower temperatures, the L/V ratio is  $\sim 1$  suggesting that primarily two ligands are removed, and indicating the formation of bidentate-way bonded species on the silica surface. For the higher temperatures, only the monodentate bonded species (L/V =  $\sim 2$ ) are formed by the removal of one ligand out of the original three. The species are visualized using molecular modeling in 3D in the section 3.1.3.

In the literature, Rice et al.<sup>16</sup> and Nickl et al.<sup>14</sup> had bound volatilized vanadyl triisopropoxide at room temperature on silica pretreated at different temperatures. The former authors<sup>16</sup> observed vanadium surface densities of  $\sim 2.9$  and  $\sim 1.4$  at/nm<sup>2</sup><sub>sup</sub> after deposition on silica pretreated at 473 and 773 K, respectively, while the latter authors<sup>14</sup> obtained a density of  $\sim 2.3$  at/nm<sup>2</sup><sub>sup</sub> on silica pretreated at 423 K. These densities are in accordance with our results with the exception of the relatively high density obtained by Rice et al.<sup>16</sup> on silica pretreated at 473 K. This difference may be due to the lower deposition temperature (298 K) used by the authors,<sup>16</sup> which allows for some physisorption of the precursor and thus leads to a higher vanadium amount.

**DRIFTS Measurements.** To confirm the results from the chemical analyses, diffuse reflectance FTIR measurements were carried out in inert conditions after the binding of the precursor on the silica surfaces pretreated at 473, 723, 873, and 1023 K. Figure 4A presents the DRIFTS patterns in the range between 400 and 3800 cm<sup>-1</sup> of the pure silica pretreated at different temperatures. Figure 4B presents the patterns of the solids after precursor deposition at 363 K, and Figure 4C after further oxidation.

The silica pretreated at 473 K give rise to the broad IR vibrations at  $\sim 3745$  cm<sup>-1</sup> (unpaired silanols),  $\sim 3650$  cm<sup>-1</sup> (intraglobular OH) and  $\sim 3520$  cm<sup>-1</sup> (oxygen perturbed OH).<sup>28–30</sup> By increase of the pretreatment temperature from 723 to 1023 K, the condensation of silanols decreases the broad band at  $\sim 3700$  cm<sup>-1</sup> in favor of the sharpening peak at  $3745$  cm<sup>-1</sup>.<sup>28–30</sup> The formation of siloxane bridges by heating at elevated temperatures ( $> 723$  K), on the other hand, intensifies the band at  $\sim 1000$  cm<sup>-1</sup>, which overlaps the decreasing one at  $\sim 980$  cm<sup>-1</sup> due to Si–O vibration of isolated silanols.<sup>28,31,32</sup> Si–O–Si and O–Si–O stretching modes of the silica lattice give rise to the bands at  $\sim 1025$  cm<sup>-1</sup> and  $\sim 835$  cm<sup>-1</sup>, respectively.<sup>30–32</sup>

The adsorption of the precursor at 363 K onto the silica surface pretreated at between 473 and 1023 K gave rise to the C–H vibration bands of the vanadium-bound isopropoxide ligands at  $\sim 2974$ , 2932, 2882, 1467, 1452, 1381, 1367, and 1332 cm<sup>-1</sup>,<sup>16,33,34</sup> as reported above. The identical DRIFT spectra collected for the samples taken from the upper and lower parts of the silica fixed-bed confirmed the homogeneity of the

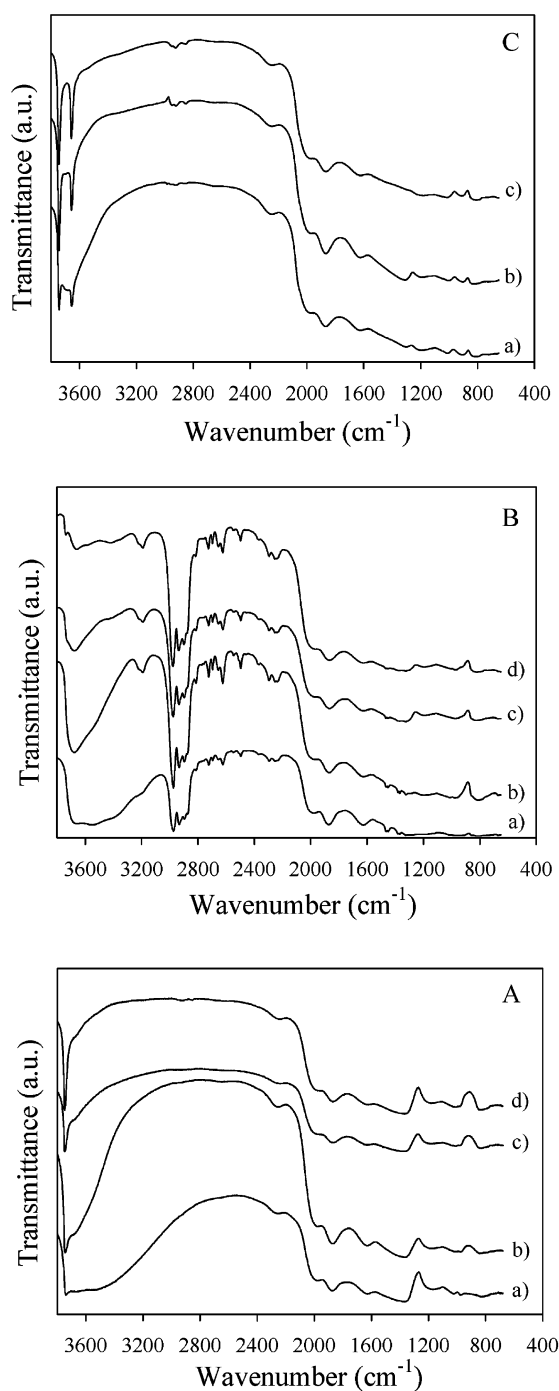


**Figure 4.** DRIFTS patterns: (A) Silica support pretreated at (a) 473 K, (b) 723 K, (c) 873 K, and (d) 1023 K. (B) After precursor deposition at 363 K on silica pretreated at (a) 473 K, (b) 723 K, (c) 873 K, and (d) 1023 K. (C) After further oxidation at 723 K (sample a) or 773 K (samples b and c) on silica pretreated at (a) 723 K, (b) 873 K, and (c) 1023 K.

deposition process throughout the support bed. Furthermore, the disappearance of the Si–OH peak at  $3745$  cm<sup>-1</sup>, in the case of the silicas pretreated at 473, 723, and 873 K (Figure 4Ba–c), indicated the saturation of the surface.<sup>11,23,26</sup> However, in the case of silica pretreated at 1023 K, a small isolated OH peak persisted after the excess precursor gas feeding through the support bed (Figure 4B, sample d). The highly identical vanadium amounts ( $< \pm 0.05$  at/nm<sup>2</sup><sub>sup</sub>) throughout the fixed-bed of support nevertheless indicated a good macroscopic homogeneity<sup>11</sup> and excluded the excess decomposition of precursor. However, as the silica support dehydroxylated at 1023

K contains an increasing amount of highly reactive siloxane bridges,<sup>11,28,31,32</sup> these Si—O—Si linkages could have participated in the reaction process by dissociation. The dissociation of the bridges could have been caused by their reaction with either the precursor, as shown in the case of alkoxysilane precursors,<sup>30,36</sup> or with the reaction product 2-propanol, as demonstrated for methanol.<sup>37</sup> However, further studies, e.g., measurements of 2-propanol adsorption in the ALD reactor in the same deposition conditions and application of silica with a greater amount of siloxane bridges i.e., silica pretreated at higher (1073–1273 K) temperatures, are needed to verify these hypotheses.

The DRIFTS patterns of the solids were also collected after calcination, and they are reported in Figure 4C. The intensities of the peaks at  $\sim 3745\text{ cm}^{-1}$  and at  $3660\text{ cm}^{-1}$  ( $\nu(\text{O—H})$  attached to vanadia surface species)<sup>9</sup> increased gradually when the silica pretreatment temperature was increased from 723 to 1023 K (Figure 4C, samples a–c). Due to the interfering strong absorption of the silica support in the vibration region below  $1000\text{ cm}^{-1}$ ,<sup>16,38</sup> the structure of the surface vanadia species ( $\text{V=O}$  and  $\text{V—O}$  vibrations) was investigated in detail by more appropriate Raman spectroscopy technique, as reported later in the section for physicochemical characterization (3.2.4.).

Moreover, the influence of the quantity of silica support (5–11 g) on the ALD growth was studied at 383 K. It was observed that even at this low reaction temperature, when the volume of silica pretreated at 873 K was maximized in the quartz reaction chamber (11 g) and an excess of precursor ( $\sim 2.7\text{ mmol/g}_{\text{sup}}$ ) was used, the highly reactive vanadyl alkoxide precursor started to slightly decompose on the top of the thick support bed. This was observed from the deeper coloring of the top of the support bed. However, this phenomenon was typical only for this alkoxide precursor; as in the case of the corresponding, more stable titanium isopropoxide  $\text{Ti}(\text{OPr}^i)_4$ , the increasing of the support amount did not affect the controlled growth process.<sup>39</sup>

**3.1.3. Surface Structures of the Precursor Complex After Gas–Solid Reaction.** Within the controlled atomic layer deposition range at temperatures between 363 and 393 K, the ligand/vanadium ratio ( $L/V$ ) of the surface complex attached onto silica pretreated at 873 K decreased from 1.7 to 1.4. In general, when the chemisorption was carried out at 363 K, the  $L/V$  ratio calculated was  $\sim 1$  for the silicas pretreated at low temperatures (473 or 723 K) and  $\sim 2$  for the silicas pretreated at high temperatures (873 or 1023 K). These observations are in agreement with the literature data for the gas-phase reaction of vanadyl triethoxide  $\text{VO}(\text{OEt})_3$  at 423 K with silica pretreated at 523 and 773 K.<sup>9</sup> In this study of Inumaru et al.,<sup>9</sup> it was suggested that the surface species on silica pretreated at 523 K had principally an  $L/V$  ratio of  $\sim 1$  indicating a bidentate nature of the alkoxide surface complex. A formation of both monodentate ( $L/V = \sim 2$ ) and bidentate ( $L/V = \sim 1$ ) bonded species was observed on silica pretreated at 773 K.<sup>9</sup>

However, Rice et al.<sup>16</sup> showed that when the gas-phase deposition of  $\text{VO}(\text{OPr}^i)_3$  on silica was carried out at room temperature, only one  $\text{PrOH}$  was liberated during grafting (i.e.,  $L/V = 2$ ), independently of the pretreatment temperature of the support (298, 473, or 773 K). This discrepancy may be due to the different deposition temperatures used (viz., 363 K in this study and 298 K in the study of Rice et al.).<sup>16</sup> The higher deposition temperature increased the reactivity of the precursor,<sup>12</sup> i.e., favored the reaction of the precursor with two surface sites instead of one, whereas the low deposition temperature may have allowed also some physisorption of the vanadyl triisopropoxide.

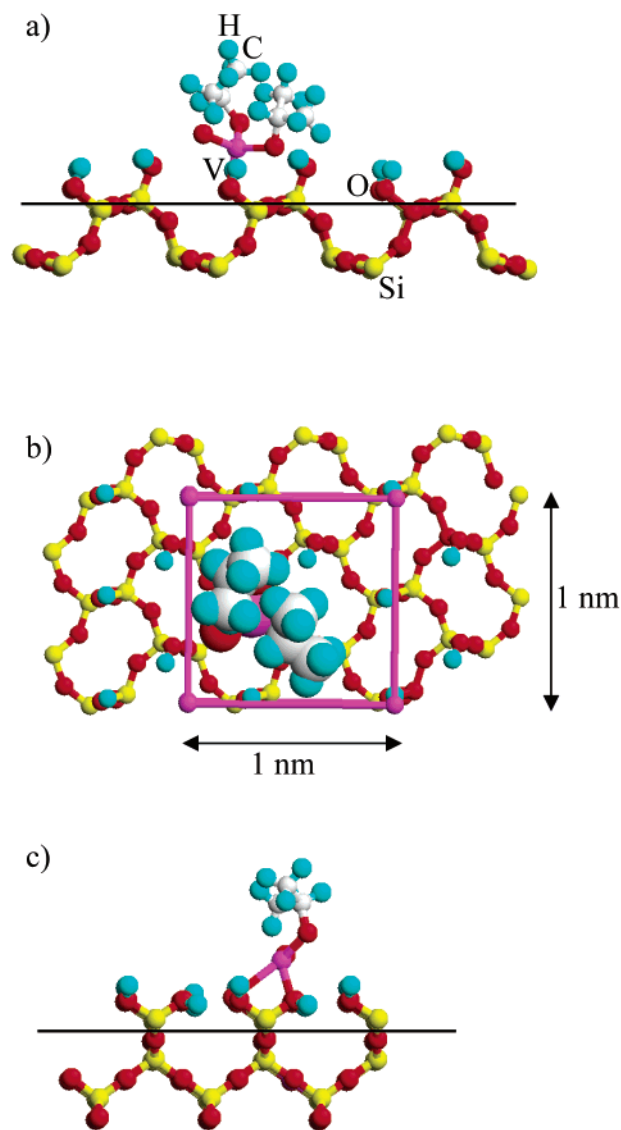


**Figure 5.** Binding of  $\text{VO}(\text{OPr}^i)_3$  on silica  $\beta$ -cristobalite surfaces: (a), (b) monodentate bonding ( $L/V = 2$ ) on (111) surface and (c) bidentate bonding ( $L/V = 1$ ) on (100) surface.

A theoretical confirmation of the presence of mono- and bidentate bonded species was achieved by means of molecular modeling in 3D. The general illustrations of surface complexes with remaining one or two triisopropoxide ligands ( $L/V = 1$  or 2, respectively) are presented in Figure 5. The (111) and (100) faces of  $\beta$ -cristobalite have often been used as models for the amorphous silica surface.<sup>9,40,41</sup> The (111) face shows the distribution of isolated, free silanol groups, with a separation between the two nearest groups of  $\sim 5\text{ \AA}$ .<sup>9,40,41</sup> The (100) face exposes the geminal OH groups (i.e., two hydroxyl groups attached to the same Si atom). The interspace between the rows of paired hydroxyl groups on the (100) face is  $\sim 5\text{ \AA}$ ,<sup>40</sup> whereas the shortest distance between the groups is  $\sim 2.5\text{ \AA}$ .<sup>9</sup> As the distance order between oxygen atoms in the  $\text{O—V—O}$  bonds of a vanadyl alkoxide molecule has been reported to be  $\sim 2.5\text{ \AA}$ ,<sup>9</sup> the precursor can react on the (111) face with only one isolated OH group, upon releasing one isopropoxide ligand ( $L/V = 2$ ) (Figure 5a). Figure 5b displays well the size of the precursor with  $L/V = 2$  on the silica surface. The vicinity of the OH groups on the (100) face allows, however, both the monodentate ( $L/V = 2$ ) and bidentate ( $L/V = 1$ ) (Figure 5c) binding of the precursor.<sup>9</sup> The reaction with three OH groups by a release of



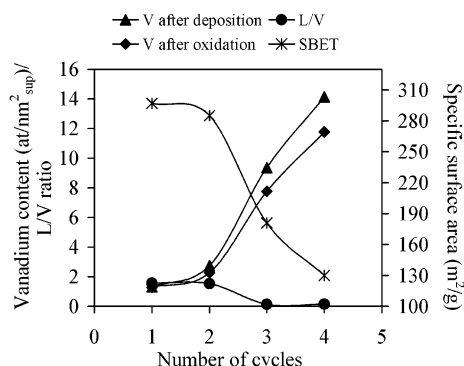


**Figure 6.** Influence of the cycle number on the average vanadium contents (after deposition and oxidation), ligand/vanadium ratio (after deposition) and  $S_{\text{BET}}$  (after oxidation) when the precursors  $\text{VO}(\text{OPr})_3$  and oxygen are bound onto silica pretreated at 873 K.

all the three ligands ( $\text{L}/\text{V} = 0$ ) is not possible due to the steric effects.<sup>9</sup> These observations thus confirm the experimental results determined in the earlier paragraphs (3.1.1–3.1.2.) from the chemical analysis data.

**3.1.4. Application of Several Precursor-Oxygen Cycles on Silica Pretreated at 873 K.** One and Two ALD Cycles. Four successive vanadium precursor–calcination cycles on silica pretreated at 873 K were carried out at a deposition temperature of 383 K to study the changes in the reaction mode when increasing the vanadium content in the catalysts. The vanadium concentrations after deposition/oxidation, ligand/vanadium ( $\text{L}/\text{V}$ ) ratios after deposition and specific surface areas ( $S_{\text{BET}}$ ) of the calcined catalysts are presented in Figure 6 as functions of the cycle number. When using the precursor in excess, a surface-site-controlled ALD growth was possible during the first and second cycles, leading to vanadium concentrations of 1.3 (first cycle) and 2.6 or 2.3  $\text{at}/\text{nm}^2_{\text{sup}}$  (second cycle) after deposition or oxidation, respectively.<sup>26</sup> The  $\text{L}/\text{V}$  ratio, calculated after deposition, was  $\sim 1.5$  both after the first and second cycles, indicating no major change in the binding and a general loss of one or two ligands when forming the surface complex.

The BET surface areas of the calcined catalysts were 297 and 285  $\text{m}^2/\text{g}$ , after the first and second cycle, respectively (Figure 6). The values stayed high as compared to  $S_{\text{BET}}$  values of 274 and 256  $\text{m}^2/\text{g}$  for similar catalysts onto silica ( $S_{\text{BET}} = 332 \text{ m}^2/\text{g}$ ), grafted in vanadyl triisopropoxide liquid phase and containing 0.9 and 2.6  $\text{at}/\text{nm}^2_{\text{sup}}$  of vanadium, respectively.<sup>10</sup> This better result obtained using the gas-phase deposition route can be mainly due to the absence of solvent effects in the ALD procedure.<sup>12</sup> DRIFT spectroscopy data showed for the calcined, one- and two-cycle ALD catalysts the formation of vanadia surface species ( $3660 \text{ cm}^{-1}$ )<sup>9</sup> and the partial regeneration of the isolated  $\text{Si}-\text{OH}$  groups ( $3745 \text{ cm}^{-1}$ ).<sup>9,28</sup> The intensity of these peaks diminished with the increasing vanadium content. The relative dispersion of the vanadia species was high because no XRD peaks due to  $\text{V}_2\text{O}_5$  crystallites ( $d > \sim 4\text{--}5 \text{ nm}$ )<sup>42</sup> were detected these catalysts.

**Three and Four ALD Cycles.** In the literature, the experimental monolayer dispersion determined by Raman spectroscopy has been reported to be  $\sim 2.6 \text{ at}/\text{nm}^2_{\text{sup}}$  for silica-supported vanadia.<sup>10,13</sup> In consequence, after the second deposition cycle and when the quantity of vanadium oxide was near this maximum coverage, the evidently catalytically very active surface started to partly decompose the precursor even at the low deposition temperature employed (383 K). The growth during the third and fourth depositions was no longer surface controlled, and the remarkably increasing vanadium content

**TABLE 1: Chemical Analysis and  $\text{N}_2$  Adsorption Results of Silica Supports and ALD and Impregnated Vanadia Catalysts**

sample <sup>a</sup>	vanadium amount		$S_{\text{BET}}$	pore vol	avg
	(wt-%)	( $\text{at}/\text{nm}^2_{\text{sup}}$ )	( $\text{m}^2/\text{g}$ )	( $\text{cm}^3/\text{g}$ )	pore diam (nm)
$\text{SiO}_2$ 723	<i>b</i>	<i>b</i>	305	1.2	19–20
A-1VS-723	3.8	1.6	295	1.2	21
$\text{SiO}_2$ 873	<i>b</i>	<i>b</i>	301	1.2	19–20
A-1VS-873	2.9	1.2	297	1.2	20
A-2VS-873	5.2	2.3	285	1.2	20
I-1VS-873	3.6	1.5	286	1.2	20
I-2VS-873	5.8	2.5	272	0.9	19
$\text{SiO}_2$ 1023	<i>b</i>	<i>b</i>	286	1.1	19–20
A-1VS-1023	2.4	1.0	286	1.1	19

<sup>a</sup> A = ALD, I = impregnation, 723, 873, 1023 = pretreatment temperature of the support in K. <sup>b</sup> Negligible or zero.

(Figure 6) was strongly dependent on the amount of precursor loaded in the reactor ( $\sim 2.5 \text{ mmol}/\text{g}_{\text{sup}}$ ). The average  $\text{L}/\text{V}$  ratios decreased to values near zero, indicating precursor decomposition (Figure 6). The decomposition was also shown from the decrease in the isopropoxide C–H vibrations ( $2882$ ,  $2932$ , and  $2974 \text{ cm}^{-1}$ )<sup>33,34</sup> in DRIFTS patterns collected after deposition.

As can be seen in Figure 6, a marked decrease in specific surface area was observed for the calcined catalysts of three and four vanadia cycles.<sup>26</sup> The pore volume of the support was affected as well, decreasing from 1.2 to 0.6  $\text{cm}^3/\text{g}$  after the fourth cycle. Furthermore, characteristic XRD peaks of  $\text{V}_2\text{O}_5$  were detected in the diffraction pattern at e.g.,  $2\theta = 15.4^\circ$ ,  $20.3^\circ$ ,  $21.7^\circ$ ,  $26.2^\circ$ ,  $31.1^\circ$ ,  $32.4^\circ$ , and  $34.3^\circ$ ,<sup>43</sup> in the three- and four-cycle catalysts.

This study of sequential cycle deposition indicates the importance of the precursor when synthesizing  $\text{V}_2\text{O}_5/\text{SiO}_2$  catalysts in a gas-phase. When the goal is the gas-phase deposition of high coverage of vanadium oxide, other volatile precursors such as vanadium(IV) and vanadyl(V) chlorides  $\text{VCl}_4$  and  $\text{VOCl}_3$ , respectively, could be an alternative, because they are more resistant than alkoxides to contact with a catalytically active surface.<sup>44</sup> However, because the chloride-containing precursors are corrosive, etch the deposited surface effectively, and often leave Cl impurities in the sample,<sup>29</sup> the alkoxide precursors are ideal for the growth of low loading, from sub- to monolayer vanadia catalysts,<sup>5,9</sup> preferred for several catalytic reactions.<sup>7</sup>

### 3.2. Physicochemical Characterization of the Catalysts.

**3.2.1. Vanadium Analysis and Surface Area/Porosity Measurements.** The physicochemical properties of the ALD catalyst prepared by applying one reaction cycle on silica pretreated at 723 and 1023 K and up to two reaction cycles (i.e., controlled preparation) on silica pretreated at 873 K were examined further. Two aqueous-phase impregnated catalysts corresponding to the ALD catalysts on silica 873 K were characterized for comparison. The results from the vanadium content determinations,  $\text{N}_2$  adsorption, and XPS measurements for the silica support and vanadia catalysts are summarized in Table 1. In the sample labels,  $x$ - $y$ VS- $z$ ,  $x$  corresponds to the preparative method (A = ALD or I = impregnation),  $y$  to the ALD cycle number ( $y = 1$  or 2) and  $z$  to the silica pretreatment temperature ( $z = 723$ , 873 or 1023 K) applied.

As discussed in the previous paragraph, one precursor binding-oxidation ALD cycle onto silica 723 and 1023 K resulted in surface concentrations of 1.6  $\text{at}/\text{nm}^2_{\text{sup}}$  (3.8 wt-%) and 1.0  $\text{at}/\text{nm}^2_{\text{sup}}$  (2.4 wt-%), respectively (Table 1). The first and second ALD cycle on silica 873 K gave rise to the vanadium amounts of 1.2  $\text{at}/\text{nm}^2_{\text{sup}}$  (2.9 wt-%) and 2.3  $\text{at}/\text{nm}^2_{\text{sup}}$

(5.2 wt-%), respectively. These AL depositions of vanadia caused only a small decrease (<6%) in the specific surface area of the support (Table 1). However, when the addition of corresponding amounts of vanadia on silica 873 K was done by aqueous impregnation, the  $S_{\text{BET}}$  values of the catalysts were ~10% inferior than that of the support, and a greater pore volume diminution was observed at higher vanadium content (Table 1).

**3.2.2. X-ray Diffraction.** X-ray diffraction was used to detect  $\text{V}_2\text{O}_5$  crystallites large enough, that is with a diameter higher than ~4–5 nm,<sup>42</sup> on the amorphous silica support. The vanadia catalysts prepared by ALD on silica pretreated at 723, 873, and 1023 K showed no XRD-detectable peaks. However, a weak  $\text{V}_2\text{O}_5$  peak at  $2\theta = 26.2^\circ$  was detected for the impregnated samples I-1VS-873 and I-2VS-873 (XRD spectra not presented).<sup>43</sup>

**3.2.3. X-ray Photoelectron Spectroscopy.** The influence of the preparative method and the amount of vanadium on the relative dispersion of vanadium oxide species and the oxidation state of vanadium have been examined by X-ray photoelectron spectroscopy. Only the one- and two-cycle ALD and impregnated samples on silica 873 K have been included in the study.

Andersson<sup>45</sup> has examined several vanadium oxides by XPS and tabulated their binding energies of  $\text{V}2\text{p}^{3/2}$  signals by referring the spectra to the  $\text{O}1\text{s}$  line at 529.6 eV. Because the calibration in this study designates the  $\text{O}1\text{s}$  signal of  $\text{V}_2\text{O}_5$  (Aldrich, purity 99.99%) at 529.9 eV (i.e., allows a shift of 0.3 eV in  $\text{V}2\text{p}^{3/2}$  peak positions toward higher binding energies)<sup>46</sup> the reference  $\text{V}2\text{p}^{3/2}$  signals for  $\text{V}_2\text{O}_5$ ,  $\text{V}_6\text{O}_{13}$ ,  $\text{V}_2\text{O}_4$ , and  $\text{V}_2\text{O}_3$  could be assigned to 516.9, 516.6, 515.9, and 515.7 eV, respectively.

The binding energies (BE) for the  $\text{V}2\text{p}^{3/2}$  line were ~516.7 and ~517.0 eV for the low and high vanadia loaded catalysts, respectively. The values indicate that the vanadia surface species were fully oxidized (oxidation state  $\text{V}^{5+}$ ) in the latter samples and that they could be slightly reduced to the states between  $\text{V}^{4+}$  and  $\text{V}^{5+}$  in the former samples.<sup>45,46</sup> It should, however, be noticed that the observed shift (0.3 eV) is practically within the limit of experimental errors. The slight reduction of the more reducible, less vanadia-containing samples<sup>47</sup> A-1VS-873 and I-1VS-873, is mainly due to the exposure of the catalysts to X-radiation in a UHV environment during the data acquisition<sup>48</sup> and, according to the literature,<sup>46</sup> also possibly to the  $\text{NH}_3$  adsorption performed at 353 K before the XPS measurements. This latter hypothesis is, however, not very probable, because the binding energies measured before the adsorption of  $\text{NH}_3$  were practically the same.

The contributions in percentage of the M–O components ( $\text{M} = \text{V}$  or  $\text{Si}$ ) in the catalysts, calculated from the spectra corresponding to  $\text{O}1\text{s}$  line, are presented in Figure 7 together with the relative V/Si atomic ratios, calculated from the XPS or chemical analysis (CA) data for the vanadia catalysts.

The appearance of the  $\text{O}1\text{s}$  spectra of the ALD and impregnated catalysts (not presented) was rather independent of the vanadium loading and consisted of a large band that could be divided into a band centered at ~531.0 eV (contribution ~5–10%) and at ~532.7 eV (contribution ~90–95%) (Figure 7). The maximum at higher binding energy value can be attributed to the silicon bonded oxygen in the  $\text{SiO}_2$  lattice (exact value 532.8 eV)<sup>48,49</sup> and the maximum at lower value to arise from the presence of vanadia species (value for bulk  $\text{V}_2\text{O}_5$  is 529.9 eV).

The surface V/Si atomic ratios, probing the relative vanadia species dispersion, were slightly higher for the ALD prepared

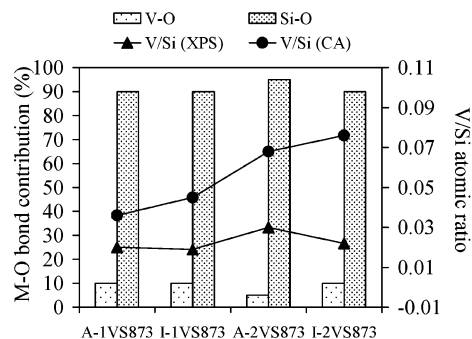


**Figure 7.** Relative contributions of the M–O components ( $\text{M} = \text{V}$  or  $\text{Si}$ ) derived from the XP spectra of  $\text{O}1\text{s}$  line together with V/Si atomic ratios from XPS and chemical (CA) analysis for the ALD and impregnated vanadia catalysts on silica pretreated at 873 K.

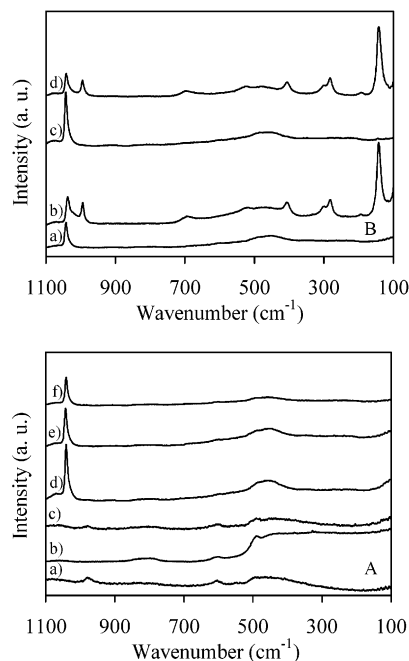


**Figure 8.** Raman spectra: (A) Dehydrated silica supports and ALD vanadia catalysts (a)  $\text{SiO}_2$  723 K, (b)  $\text{SiO}_2$  873 K, (c)  $\text{SiO}_2$  1023 K, (d) A-1VS-723, (e) A-1VS-873 and (f) A-1VS-1023. (B) Dehydrated ALD and impregnated vanadia catalysts: (a) A-1VS-873, (b) I-1VS-873, (c) A-2VS-873 and (d) I-2VS-873.

A-1VS-873 (ratio 0.020) and A-2VS-873 (0.030) catalysts than for the corresponding impregnated ones I-1VS-873 (0.019) and I-2VS-873 (0.022), as seen in Figure 7. However, these ratios were ~40–50% and ~60–70% smaller than the bulk ratios for ALD and impregnated catalysts, respectively (Figure 7). This may be due both to a bad estimation of the intensity factors of XP peaks and to the fact that a great part of vanadium is located inside of the channels or mesopores of silica, away from the detection capability (depth <~5 nm) of the XPS technique.<sup>45,49</sup>

**3.2.4. Raman Spectroscopy.** Micro-Raman spectroscopy was applied to study the nature of the vanadia species in the catalysts and to confirm the crystallinity and dispersion features observed by X-ray diffraction and photoelectron spectroscopies.

Raman spectra of silicas pretreated at 723, 873, 1023 K and those of silica-supported atomic layer deposited catalysts are presented in Figure 8A. The spectra of the one- and two-cycle ALD catalysts on silica 873 K and the corresponding impregnated catalysts are presented in Figure 8B. The samples were dehydrated at 673 K in oxygen flow before the Raman measurements.



The silica supports pretreated at different temperatures (Figure 8A, samples a–c), showed broad Raman features at wavenumbers from 400 to 470  $\text{cm}^{-1}$  and from 750 to 850  $\text{cm}^{-1}$  due to the siloxane bending  $\delta(\text{Si-O-Si})$  and stretching  $\nu_s(\text{Si-O-Si})$  modes<sup>10,50</sup> and at  $\sim 1050 \text{ cm}^{-1}$  due to the  $\nu_{\text{as}}(\text{Si-O-Si})$  linkages,<sup>30–32,50</sup> in accordance with the inert DRIFTS measurements. The band at  $\sim 976 \text{ cm}^{-1}$  can be assigned to the Si–O stretching mode of isolated hydroxyls.<sup>31,50,51</sup> In addition to these bands, two rather distinct features at wavenumbers 595 and 484  $\text{cm}^{-1}$  arose from the tri- and tetra cyclosiloxane rings, respectively.<sup>10,49,50</sup>

The ALD catalysts were observed to be very homogeneous as identical Raman spectra were recorded after focusing the analysis spot of the microscope at several points on the powder surface. The spectra of the catalysts on silicas pretreated at different temperatures (Figure 8A, samples d–f) showed distinct peaks at wavenumber  $\sim 1042 \text{ cm}^{-1}$  due to the stretching  $\nu(\text{V=O})$  of isolated tetracoordinated vanadate species.<sup>10,50,52</sup> The literature references recite that these isolated  $\text{VO}_4$  species on silica are composed from one terminal  $\text{V=O}$  bond and from three bridging  $\text{V-O-Si}$  bonds.<sup>10,19,50,52</sup> The intensity of the peak at  $\sim 1042 \text{ cm}^{-1}$  decreased gradually with decreasing amount of vanadium (i.e., increasing pretreatment temperature of silica (Figure 8A, samples d–f)). Moreover, presumably either the silica carrier or noncrystallized vanadia gave rise to a broad, rather intense band at  $\sim 440 \text{ cm}^{-1}$  in these ALD catalysts.<sup>10</sup>

The differences in structure and coordination of vanadia species between ALD and liquid-phase impregnated catalysts can be specifically pointed out based on the averaged spectra in Figure 8B. For A-1VS-873 (Figure 8B, sample a) and A-2VS-873 (Figure 8B, sample c) catalysts, intense peaks at 1042 and 1043  $\text{cm}^{-1}$ , respectively, and broad bands at  $\sim 440 \text{ cm}^{-1}$  were detected. The intensity of the monomeric species peak at  $\sim 1042 \text{ cm}^{-1}$  was doubled when the amount of vanadium was increased from 1.2  $\text{V at/nm}_{\text{sup}}^2$  in A-1VS-873 to 2.3  $\text{V at/nm}_{\text{sup}}^2$  in A-2VS-873.

For the two-cycle ALD catalyst, A-2VS-873, also a trace quantity of  $\text{V}_2\text{O}_5$  could be revealed by scrutinizing with the sensitive Raman spectroscopy<sup>49</sup> visible as a very weak feature at 143  $\text{cm}^{-1}$  in Figure 8B, sample c.<sup>10,53</sup> This observation confirms the maximum dispersion of vanadia at  $\sim 2.3 \text{ V at/nm}_{\text{sup}}^2$ . Similarly, Gao et al.<sup>10</sup> have determined by Raman spectroscopy an experimental monolayer coverage of  $\sim 2.6 \text{ V at/nm}_{\text{sup}}^2$  for the silica-supported vanadia catalyst prepared by incipient-wetness impregnation with a 2-propanol solution of vanadyl triisopropoxide. On the other hand, Das et al.<sup>53</sup> have observed for the catalyst prepared with vanadyl triisopropoxide in methanol the formation of crystalline  $\text{V}_2\text{O}_5$  on the high surface area silica already at a coverage of 1.6  $\text{V at/nm}_{\text{sup}}^2$ .

The two rather heterogeneous liquid-phase impregnated samples I-1VS-873 (Figure 8Bb) and I-2VS-873 (Figure 8Bd) prepared for comparison showed typical crystalline  $\text{V}_2\text{O}_5$  bands at wavenumbers of  $\sim 143, 194, 282, 301, 407, 470, 515, 694$ , and 994  $\text{cm}^{-1}$ .<sup>10,44,52,54</sup> Especially the bands at  $\sim 143$  (skeletal vibration of  $\text{V}_2\text{O}_5$ ), 282, 407, and 994  $\text{cm}^{-1}$  ( $\nu_s(\text{V=O})$  in multilayer structure)<sup>5,10,51,52,54</sup> were very intense and narrow. On the other hand, the broadness of bands at 470  $\text{cm}^{-1}$  has been discussed to be due to poorly crystallized vanadia.<sup>10</sup> This early formation of vanadium pentoxide crystals, e.g., at concentrations of  $\sim 1.0 \text{ V at/nm}_{\text{sup}}^2$ , is often observed in the literature to occur for the silica-supported catalysts prepared from the solutions of vanadium oxalate complex.<sup>54</sup> Moreover, the isolated species gave rise to the peak at 1037  $\text{cm}^{-1}$  for I-1VS-873 (Figure 8Bb), of which the intensity decreased

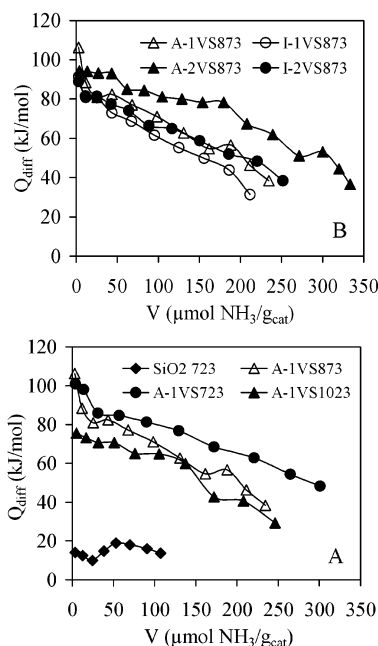


**Figure 9.** Differential heat of ammonia adsorption at 353 K as a function of ammonia coverage: (A) Adsorption on silica support pretreated at 723 K and ALD catalysts on silica pretreated at 723, 873, and 1023 K. B. Adsorption on ALD and impregnated vanadia catalysts on silica pretreated at 873 K.

and position shifted slightly at higher wavenumber (1042  $\text{cm}^{-1}$ ) as the vanadium content increased (I-2VS-873, Figure 8B, sample d).

The impregnated and ALD-prepared, silica-supported samples (Figure 8A, samples d–f, Figure 8B, samples a–d) showed also a broad band at  $\sim 1070 \text{ cm}^{-1}$  due to perturbed  $\text{Si-O}^-$  and  $\text{Si}(\text{O}^-)_2$  vibrations indicating that the  $\text{V-O-Si}$  bridging bonds are formed by breaking  $\text{Si-O-Si}$  bridges.<sup>10,53</sup> The decrease in number of cyclosiloxane rings was also observed from the weakening of the band at  $\sim 595 \text{ cm}^{-1}$ .<sup>10,55</sup> The dissociation of strained siloxane bridges has also been suggested in studies by Blümel,<sup>36</sup> using solid-state NMR, and Dubois et al.,<sup>30</sup> using FTIR of alkoxyisilane reactions with high surface area silica, dehydroxylated at 873 and 1250 K, respectively. On the other hand, Chuang et al.<sup>56</sup> reported that siloxane linkages formed during pretreatment at temperatures above 773 K were highly reactive toward molecules such as water or ammonia, which could have caused the cleaving of siloxane bridges during the calcination of our catalysts impregnated with an ammonium metavanadate solution.

**3.3. Acidity of the Catalysts.** The acidity of the catalysts in the form of surface reactivity toward ammonia was evaluated by two techniques: adsorption microcalorimetry to obtain the total number, the strength and the strength distribution of acid sites and X-ray photoelectron spectroscopy to determine the nature (Lewis/Brønsted) of the adsorbed species and to have an indication of the number of medium strength and strong surface acid sites.<sup>24,25</sup>

**3.3.1. Adsorption Microcalorimetry.** The differential heats ( $Q_{\text{diff}}$ ) of ammonia adsorption at 353 K on silica support and ALD vanadia catalysts are presented in Figure 9A with increasing surface coverage. The comparison of the  $Q_{\text{diff}}$  values of ALD and impregnated vanadia catalysts on silica pretreated at 873 K is done in Figure 9B. When nonacidic silica support presented only plateau at low  $Q_{\text{diff}}$  value  $< 20 \text{ kJ/mol}$  (Figure 9A),<sup>57,58</sup> the addition of vanadia by impregnation or ALD created essentially rather weak surface acid sites with evolved heats

**TABLE 2: Calorimetric and Volumetric Data Obtained from Ammonia Adsorption and Desorption at 353 K**

sample	$Q_{\text{init}}^a$ (kJ/mol)	$V_T^b$ ( $\mu\text{mol NH}_3/\text{g}_{\text{cat}}$ )	$V_{\text{irr}}^c$ ( $\mu\text{mol NH}_3/\text{g}_{\text{cat}}$ )	$Q_{\text{int}}^d$ (J/g <sub>cat</sub> )	acid site number ( $\mu\text{mol NH}_3/\text{g}_{\text{cat}}$ )		
					60 < $Q$ < 80 kJ/mol	80 < $Q$ < 100 kJ/mol	100 < $Q$ < 120 kJ/mol
SiO <sub>2</sub> 723	14	66	28	1	<i>e</i>	<i>e</i>	<i>e</i>
A-1VS-723	101	213	24	17	134	94	7
A-1VS-873	106	156	18	12	80	48	6
A-2VS-873	94	225	27	18	116	129	<i>e</i>
I-1VS-873	91	139	21	10	76	27	<i>e</i>
I-2VS-873	89	172	37	12	112	31	<i>e</i>
A-1VS-1023	76	164	24	12	137	<i>e</i>	<i>e</i>

<sup>a</sup> Initial heat of adsorption. <sup>b</sup> Total adsorbed volume at 27 Pa. <sup>c</sup> Irreversibly adsorbed volume at 27 Pa. <sup>d</sup> Integral heat of adsorption at 27. <sup>e</sup> Negligible or zero.

( $Q$ ) between 40 and 100 kJ/mol (Figure 9A and 9B). The differential heat of adsorption curves in Figure 9A and the detailed distribution of the acid site strengths tabulated in Table 2 show that the acidic character of the ALD catalysts on silica pretreated at different temperatures strengthened gradually with an increasing amount of vanadia. The parallel  $Q_{\text{diff}}$  curves of A-1VS-723 and A-1VS-1023 indicate that the number and strength of acid sites in these catalysts are altered in the same manner (Figure 9A). Whereas only a difference in the strength of acid sites is distinguished between A-1VS-873 and A-1VS-1023, the number of acid sites also differs between A-1VS-723 and A-1VS-873 (Figure 9A).

For the ALD and impregnated catalysts on silica pretreated at 873 K, the  $Q_{\text{diff}}$  values versus ammonia uptake revealed the importance of the preparative method on the acidity of the catalysts (Figure 9B). The good dispersion of the ALD catalysts yielded higher evolved heats and greater number and strength of acid sites. Indeed, the catalysts A-1VS-873 and I-2VS-873 displayed nearly identical calorimetric curves (Figure 9B) although the latter sample contained twice as much vanadium. Moreover, the number of acid sites (in  $\mu\text{mol NH}_3/\text{g}_{\text{cat}}$ ) which adsorb ammonia within a given heat interval ( $\Delta = 20$  kJ/mol) between 60 and 120 kJ/mol (Table 2) was always greater for the corresponding ALD sample. The progressively decreasing curves with the coverage (Figure 9B) for A-1VS-873, I-1VS-873 and I-2VS-873 indicate heterogeneity in the acid site distribution. However, more homogeneous distribution with a plateau at 90 kJ/mol is observed for A-2VS-873.

As can be seen from the calorimetric data in Table 2, the initial heats ( $Q_{\text{init}}$ ) of ammonia adsorption of the catalysts were slightly dependent on the vanadia coverage and on the preparative method being rather constant at between  $\sim 80$  and  $\sim 110$  kJ/mol. The irreversibly adsorbed amounts ( $V_{\text{irr}}$ ) illustrating the number of strong acid sites<sup>24,25</sup> were low  $\sim 20$ – $40$   $\mu\text{mol NH}_3/\text{g}_{\text{cat}}$  for all of the catalysts. The integral heats ( $Q_{\text{int}}$ ), corresponding to the total heat evolved after adsorption at 27 Pa,<sup>24,25</sup> increased from  $\sim 10$  to  $\sim 20$  J/g<sub>cat</sub> when the adding of higher amounts of vanadia was done by ALD but stayed rather constant at  $\sim 10$  J/g<sub>cat</sub> when the addition was effected by impregnation (Table 2).

The total number of acid sites ( $V_T$  values) measured from the adsorption isotherms at a pressure of 27 Pa, decreased in the order A-2VS-873 > A-1VS-723 > I-2VS-873 > A-1VS-1023 > A-1VS-873 > I-1VS-873 > SiO<sub>2</sub> (Table 2). The ammonia uptakes normalized to the same vanadium surface density were  $\sim 30\%$  greater for the ALD samples A-1VS-873 and A-2VS-873 than for the corresponding impregnated samples I-1VS-873 and I-2VS-873, respectively, this being in agreement with our earlier microcalorimetric studies of ammonia adsorption on similar, ALD and impregnated V<sub>2</sub>O<sub>5</sub>/SiO<sub>2</sub> catalysts.<sup>58</sup>

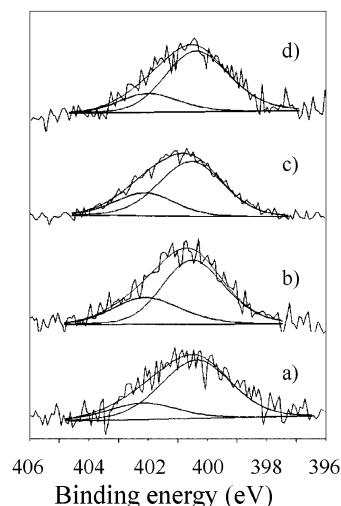


**Figure 10.** N1s XPS patterns obtained after ammonia adsorption and desorption at 353 K on ALD and impregnated vanadia catalysts: (a) A-1VS-873, (b) I-1VS-873, (c) A-2VS-873, and (d) I-2VS-873.

**3.3.2. Adsorption X-ray Photoelectron Spectroscopy.** The presence and nature of medium strength and strong surface acid sites of the ALD and impregnated samples on silica pretreated at 873 K have been studied by adsorption X-ray photoelectron spectroscopy. The XPS method of base molecule adsorption has been applied in combination with IR technique<sup>59</sup> or with adsorption microcalorimetry<sup>24,60</sup> for the quantitative and qualitative investigation of the acidic properties of zeolites and oxides. The acidic species formed upon adsorption of nitrogen containing base (e.g. NH<sub>3</sub>, pyridine, pyrrole) can be identified, and their concentration is able to be determined from the binding energy position and intensity of the N1s line, respectively.<sup>24,59,60</sup> By the ammonia adsorption XPS technique, only medium strength and strong acid sites can be detected as ammonia desorbs from the weak acid sites in ultrahigh vacuum operating conditions of XPS.<sup>24,59</sup>

The XPS spectra of N1s line obtained for the ALD and impregnated samples on silica pretreated at 873 K after NH<sub>3</sub> adsorption and desorption at 353 K are presented in Figure 10. The relative contributions of the acid sites (Lewis or Brønsted) calculated from these photoelectron spectra are shown with the surface nitrogen/vanadium (N/V) atomic ratios in Figure 11. The data of pure silica was omitted from the figures as being nonacidic; it did not adsorb ammonia in UHV conditions.

As seen in Figure 10, the broad XPS spectra of the N1s line of the ALD samples could be divided into two components at  $\sim 400.5$  and  $402.2$  eV (Figure 10, samples a and c). The former bands ( $400.5 \pm 0.1$  eV) are assigned in the literature to nitrogen which is coordinatively bonded to Lewis acid sites and the latter (402.2 eV) to the reaction of ammonia with

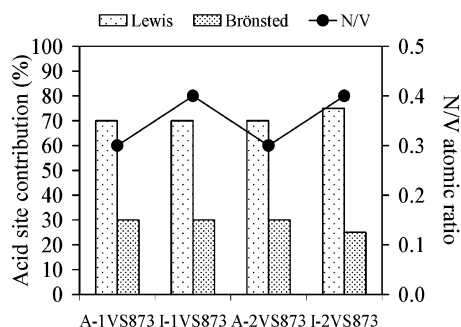


**Figure 11.** Relative contributions of the acid site components derived from the XP spectra of N1s line together with the surface N/V atomic ratios for the ALD and impregnated vanadia catalysts on silica pretreated at 873 K.

Brønsted acid sites.<sup>24,59</sup> The relative percentage ratios of the Lewis and Brønsted components are 70%/30% for the two samples (Figure 11).

The impregnated catalysts I-1VS-873 and I-2VS-873 showed also both Lewis ( $\sim 400.6$  eV) and Brønsted ( $\sim 402.1$  eV) acid site contributions, as seen in Figure 10, samples b and d. The relative concentrations of Lewis and Brønsted acid sites of the catalysts were in the scale of 70–75% and 25–30%, respectively (Figure 11). The creation of both Lewis and Brønsted acid sites upon adding vanadia at  $\sim 0.9$ – $4.1$   $\text{at}/\text{nm}^2_{\text{sup}}$  loading on silica has been shown previously in the literature.<sup>57</sup>

The slight reduction of surface vanadia species due to the UHV conditions<sup>48</sup> and ammonia adsorption,<sup>46</sup> as discussed in the XPS structural characterization paragraph (3.2.3.), might have decreased in concentration the surface Brønsted acid sites of the catalysts.<sup>7</sup> However, in another study,<sup>61</sup> we have investigated the acidity of similar ALD and impregnated, silica supported vanadia catalysts ( $1.5$ – $3.1$   $\text{at}/\text{nm}^2_{\text{sup}}$ ) by ammonia adsorption XPS and by infrared spectroscopy of pyridine adsorption. The purpose of this two-method study was to compare the acidity results obtained by a surface (XPS) and a bulk (IR) technique and to see the extent of the reduction phenomenon. Similar qualitative acid site distributions (70–75% Lewis sites, 25–30% Brønsted sites) were observed for these samples, indicating that the vanadia/silica catalysts had rather similar surface and bulk acid site compositions and that the slight surface species reduction had no significant effect on the acidic properties.<sup>61</sup>

The N/V atomic ratios obtained by XPS illustrate the number of medium strength and strong surface acid sites on which the probe molecule  $\text{NH}_3$  is adsorbed.<sup>24</sup> The ratios were slightly greater for the impregnated catalysts than for the ALD catalysts (Figure 11). This order agrees with the tendency shown by the irreversibly adsorbed volumes  $V_{\text{irr}}$  (Table 2), which correspond to the number of strong sites. Comparatively to the  $V_{\text{irr}}$ , however, it appears that N/V ratios for A-2VS-873 and I-2VS-873 are slightly too small in comparison with the two other catalysts. This probably comes from the relative dispersion of vanadium which is better after one cycle than after two cycles (Figure 11) and thus from a larger proportion of surface vanadium.

#### 4. Conclusions

Vanadyl triisopropoxide precursor was verified to be an appropriate precursor for the synthesis of highly dispersed  $\text{V}_2\text{O}_5/\text{SiO}_2$  materials by the gas-phase atomic layer deposition (ALD) technique. As shown by elemental analyses and inert atmosphere DRIFTS measurements, the surface-controlled chemisorption

of the precursor onto silica pretreated at 873 K was achieved within “the ALD temperature window”, in this case, between 363 and 393 K. The binding proceeded in a precise and reproducible way throughout the support bed and resulted in mainly bidentate surface species on silica pretreated at 473 and 723 K and mainly monodentate species on silica pretreated at 873 and 1023 K. The growth led to vanadium densities of  $\sim 2.0$ ,  $\sim 1.6$ ,  $\sim 1.4$ , and  $\sim 1.1$   $\text{V}/\text{nm}^2_{\text{sup}}$  on silica pretreated at 473, 723, 873, and 1023 K, respectively. However, the highly reactive precursor necessitated the finding of rather optimal process parameters making upscaling difficult. Due to the catalytically active nature of surface vanadia species, the deposition was possible to perform in a controlled manner only up to a near monolayer ( $\sim 2.6$   $\text{V}/\text{nm}^2_{\text{sup}}$ ) level on silica pretreated at 873 K.

The surface area and porosity of silica were only slightly affected by atomic layer deposited vanadia, and no vanadium pentoxide crystallites were observed by XRD in the catalysts. However, when the corresponding amounts of vanadium ( $1.5$  and  $2.5$   $\text{V}/\text{nm}^2_{\text{sup}}$ ) were introduced by liquid-phase impregnation of silica, the vanadia phase agglomerated decreasing the support surface area and forming crystalline  $\text{V}_2\text{O}_5$ . The differences in the surface species and crystallinity of the catalysts prepared via the gas phase or by impregnation were confirmed by Raman spectroscopy. The active phase in the ALD catalysts was homogeneous and consisted of isolated, tetracoordinated vanadate species. The species peak intensity increased gradually by increasing the vanadium coverage. In the impregnated catalysts, clear  $\text{V}_2\text{O}_5$  crystal features were detected again, together with those of the monomeric species. The X-ray photoelectron spectroscopy measurements verified the importance of the preparative method by indicating a better surface dispersion of the vanadium oxide species in the ALD catalysts than in the impregnated catalysts.

Adsorption XPS and microcalorimetry experiments showed that the acidity of the samples depended strongly on the dispersion and thereby on the mode of preparation. The vanadia addition either by impregnation or by ALD produced principally weak and medium strength surface acid sites of mainly Lewis-but also Brønsted-type in nature. For the ALD catalysts, the number and strength of surface acid sites increased gradually by increasing the vanadia surface coverage on silica. For the impregnated catalysts, the less dispersed vanadia species led to ammonia uptakes of around 30% inferior to those for the corresponding ALD catalysts.

**Acknowledgment.** The Analyses Services of IRC carried out the elemental analyses and XRD spectra acquisitions. We thank the Department of Chemistry, University of Joensuu for the access to the inert DRIFTS apparatus and Dr. Hannele Juvaste for assistance with the measurements. J.K. and E.I.I. gratefully acknowledge the funding from the Research Foundation of the Fortum Corporation.

#### References and Notes

- (1) Deo, G.; Wachs, I. E. *J. Catal.* **1994**, *146*, 323.
- (2) Wang, C.-B.; Deo, G.; Wachs, I. E. *J. Catal.* **1998**, *178*, 640.
- (3) Burcham, L. J.; Badlani, M.; Wachs, I. E. *J. Catal.* **2001**, *203*, 104.
- (4) Banares, M. A.; Gao, X.; Fierro, J. L. G.; Wachs, I. E. *Stud. Surf. Sci. Catal.* **1997**, *110*, 295.
- (5) Inumaru, K.; Misono, M.; Okuhara, T. *Appl. Catal., A* **1997**, *149*, 133.
- (6) Bond, G. C.; Tahir, S. F. *Appl. Catal., A* **1991**, *71*, 1.
- (7) Wachs, I. E.; Weckhuysen, B. M. *Appl. Catal., A* **1997**, *157*, 67.
- (8) Weckhuysen, B. M.; Keller, D. E. *Catal. Today* **2003**, *78*, 25.



- (9) (a) Inumaru, K.; Okuhara, T.; Misono, M. *J. Phys. Chem.* **1991**, 95, 4826. (b) Inumaru, K.; Okuhara, T.; Misono, M.; Matsubayashi, N.; Shimada, H.; Nishijima, A. *J. Chem. Soc., Faraday Trans.* **1992**, 88, 625. (c) Inumaru, K.; Okuhara, T.; Misono, M. *Chem. Lett.* **1990**, 7, 1207.
- (10) Gao, X.; Bare, S. R.; Weckhuysen, B. M.; Wachs, I. E. *J. Phys. Chem. B* **1998**, 102, 10842.
- (11) (a) Haukka, S.; Suntola, T. *Interface Sci.* **1997**, 5, 119. (b) Haukka, S.; Lakomaa, E.-L.; Suntola, T. *Stud. Surf. Sci. Catal.* **1998**, 120, 715.
- (12) Baltes, M.; Collart, O.; Van Der Voort, P.; Vansant, E. F. *Langmuir* **1999**, 15, 5841.
- (13) Gao, X.; Wachs, I. E. *J. Phys. Chem. B* **2000**, 104, 1261.
- (14) Nickl, J.; Dutoit, D. C. M.; Baiker, A.; Scharf, U.; Wokaun, A. *Ber. Bunsen-Ges. Phys. Chem.* **1993**, 97, 217.
- (15) Scharf, U.; Schraml-Marth, M.; Wokaun, A.; Baiker, A. *J. Chem. Soc., Faraday Trans.* **1991**, 87, 3299.
- (16) Rice, G. L.; Scott, S. L. *Langmuir* **1997**, 13, 1545.
- (17) Rice, G. L.; Scott, S. L. *Chem. Mater.* **1998**, 10, 620.
- (18) Keränen, J.; Guimon, C.; Iiskola, E. I.; Auroux, A.; Niinistö, L. *Catal. Today* **2003**, 78, 149.
- (19) Burcham, L. J.; Deo, G.; Gao, X.; Wachs, I. E. *Top. Catal.* **2000**, 11/12, 85.
- (20) Haukka, S.; Kytöki, A.; Lakomaa, E.-L.; Lehtovirta, U.; Lindblad, M.; Lujala, V.; Suntola, T. *Stud. Surf. Sci. Catal.* **1995**, 91, 957.
- (21) (a) Niinistö, L. *Curr. Opin. Solid State Mater. Sci.* **1998**, 3, 147. (b) Niinistö, L. *Proc. 23rd Int. Semicond. Conf.* **2000**, 1, 33.
- (22) Ritala, M.; Leskela, M. In *Handbook of Thin Film Materials*; Nalwa, H. S., Ed.; Academic Press: San Diego, 2002; Vol. 1, p 103.
- (23) Lakomaa, E.-L. *Appl. Surf. Sci.* **1994**, 75, 185.
- (24) (a) Guimon, C.; Gervasini, A.; Auroux, A. *J. Phys. Chem. B* **2001**, 105, 10316. (b) Auroux, A.; Gervasini, A.; Guimon, C. *J. Phys. Chem. B* **1999**, 103, 7195.
- (25) Auroux, A. *Top. Catal.* **1997**, 4, 71.
- (26) Keränen, J.; Ek, S.; Iiskola, E. I.; Auroux, A.; Niinistö, L. *Proc. 2nd Int. Conf. Silica* **2001**, 90.
- (27) Badot, J. C.; Ribes, S.; Yousfi, E. B.; Vivier, V.; Pereira-Ramos, J. P.; Baffier, N.; Lincot, D. *Electrochem. Solid-State Lett.* **2000**, 3, 485.
- (28) Van Der Voort, P.; White, M. G.; Vansant, E. F. *Langmuir* **1998**, 14, 106.
- (29) Haukka, S.; Lakomaa, E.-L.; Root, A. *J. Phys. Chem.* **1993**, 97, 5085.
- (30) Dubois, L. H.; Zegarski, B. R. *J. Am. Chem. Soc.* **1993**, 115, 1190.
- (31) Kytöki, A.; Haukka, S. *J. Phys. Chem. B* **1997**, 101, 10365.
- (32) Jung, M. *Int. J. Inorg. Mater.* **2001**, 3, 471.
- (33) (a) Schraml-Marth, M.; Wokaun, A.; Baiker, A. *J. Catal.* **1990**, 124, 86. (b) Von Witke, K.; Lachowicz, A.; Brüser, W.; Zeigan, D. *Z. Anorg. Allg. Chem.* **1980**, 465, 193.
- (34) Srinivasan, S.; Datye, A. K.; Smith, M. H.; Peden, C. H. F. *J. Catal.* **1994**, 145, 565.
- (35) Haukka, S.; Root, A. *J. Phys. Chem.* **1994**, 98, 1695.
- (36) Blümel, J. *J. Am. Chem. Soc.* **1995**, 117, 2112.
- (37) Wovchko, E. A.; Camp, J. C.; Glass, J. A., Jr.; Yates, J. T., Jr. *Langmuir* **1995**, 11, 2592.
- (38) Dunn, J. P.; Stenger, H. G., Jr.; Wachs, I. E. *Catal. Today* **1999**, 51, 301.
- (39) Keränen, J.; Guimon, C.; Iiskola, E. I.; Auroux, A.; Niinistö, L. in preparation.
- (40) Sindorf, D. W.; Maciel, G. E. *J. Am. Chem. Soc.* **1983**, 105, 1487.
- (41) Shay, T. B.; Hsu, L.-Y.; Basset, J.-M.; Shore, S. G. *J. Mol. Catal.* **1994**, 86, 479.
- (42) Keränen, J.; Auroux, A.; Ek, S.; Niinistö, L. *Appl. Catal., A* **2002**, 228, 213.
- (43) JCPDS International Centre for Diffraction Data, Powder Diffraction File, PCPDFWIN v. 2.1, 2000, card no. 85-0601.
- (44) Field, M. N.; Parkin, I. P. *J. Mater. Chem.* **2000**, 10, 1863.
- (45) Andersson, S. L. T. *J. Chem. Soc., Faraday Trans. 1* **1979**, 75, 1356.
- (46) Odriozola, J. A.; Soria, J.; Somorjai, G. A.; Heinemann, H.; Garcia de la Banda, J. F.; Lopez Granados, M.; Conesa, J. C. *J. Phys. Chem.* **1991**, 95, 240.
- (47) Koranne, M. M.; Goodwin, J. G., Jr.; Marcelin, G. *J. Catal.* **1994**, 148, 369.
- (48) Quaranta, N.; Soria, J.; Cortés Corberán, V.; Fierro, J. L. G. *J. Catal.* **1997**, 171, 1.
- (49) Gao, X.; Bare, S. R.; Fierro, J. L. G.; Banares, M. A.; Wachs, I. E. *J. Phys. Chem. B* **1998**, 102, 5653.
- (50) Jehng, J.-M.; Wachs, I. E. *Catal. Lett.* **1992**, 13, 9.
- (51) Dutoit, D. C. M.; Scheiner, M.; Fabrizioli, P.; Baiker, A. *J. Mater. Chem.* **1997**, 7, 271.
- (52) Wachs, I. E. *Catal. Today* **1996**, 27, 437.
- (53) Das, N.; Eckert, H.; Hu, H.; Wachs, I. E.; Walzer, J. F.; Feher, F. *J. J. Phys. Chem. B* **1993**, 97, 8240.
- (54) Oyama, S. T.; Went, G. T.; Lewis, K. B.; Bell, A. T.; Somorjai, G. A. *J. Phys. Chem.* **1989**, 93, 6786.
- (55) Gao, X.; Bare, S. R.; Fierro, J. L. G.; Wachs, I. E. *J. Phys. Chem. B* **1999**, 103, 618.
- (56) Chuang, I.-S.; Maciel, G. *J. Phys. Chem. B* **1997**, 101, 3052.
- (57) Le Bars, J.; Vedrine, J. C.; Auroux, A.; Trautmann, S.; Baerns, M. *Appl. Catal., A* **1992**, 88, 179.
- (58) Keränen, J.; Auroux, A.; Ek-Härkönen, S.; Niinistö, L. *Thermochim. Acta* **2001**, 379, 233.
- (59) Borade, R. B.; Adnot, A.; Kaliaguine, S. *J. Chem. Soc., Faraday Trans.* **1990**, 86, 3949.
- (60) (a) Huang, M.; Kaliaguine, S.; Auroux, A. *J. Phys. Chem.* **1995**, 99, 9952. (b) Huang, M.; Adnot, A.; Kaliaguine, S. *J. Am. Chem. Soc.* **1992**, 114, 10005.
- (61) Keränen, J.; Gervasini, A.; Guimon, C.; Auroux, A.; Niinistö, L. Unpublished results.